PALEONTOLOGY

A giant stem-group chaetognath

Tae-Yoon S. Park[1,2]*, Morten Lunde Nielsen[1,3,4], Luke A. Parry[5], Martin Vinther Sørensen[6], Mirinae Lee[1], Ji-Hoon Kihm[1,2], Inhye Ahn[1,2], Changkun Park[1], Giacinto de Vivo[7], M. Paul Smith[8], David A. T. Harper[9], Arne T. Nielsen[10], Jakob Vinther[3,11]*

Chaetognaths, with their characteristic grasping spines, are the oldest known pelagic predators, found in the lowest Cambrian (Terreneuvian). Here, we describe a large stem chaetognath, *Timorebestia koprii* gen. et sp. nov., from the lower Cambrian Sirius Passet Lagerstätte, which exhibits lateral and caudal fins, a distinct head region with long antennae and a jaw apparatus similar to *Amiskwia sagittiformis*. *Amiskwia* has previously been interpreted as a total-group chaetognathiferan, as either a stem-chaetognath or gnathostomulid. We show that *T. koprii* shares a ventral ganglion with chaetognaths to the exclusion of other animal groups, firmly placing these fossils on the chaetognath stem. The large size (up to 30 cm) and gut contents in *T. koprii* suggest that early chaetognaths occupied a higher trophic position in pelagic food chains than today.

INTRODUCTION

The Ediacaran-Cambrian transition (~540 million years ago) was marked by an exceptionally large expansion in animal diversity and disparity (*1*), which was coincident with the exploration of new regions of ecospace through deeper and more varied burrowing strategies and colonization of the water column (*2*, *3*). The causes underlying this evolutionary "explosion" remain debated, but the convergent evolution of predation and ensuing arms races (*4*) are nevertheless considered key components (*5*). Establishment of higher trophic levels would also have fueled the biological pump, by concentrating nutrients and drawing down organic carbon (*3*, *6*). The diversification of animals across the Ediacaran-Cambrian transition is increasingly recognized as a two- or three-step shift in diversity, first in the late Ediacaran "Wormworld" where simple trace fossils and tubular skeletons diversify (*7*), followed by a subsequent expansion of a more diverse biota with skeletal hard parts during the earliest Cambrian (Terreneuvian) that finally expanded in diversity markedly during the Cambrian Age 3. Chaetognaths (arrow worms) are candidates for the earliest bilaterian carnivores to have colonized the water column, as their grasping spines occur as microfossils (*Protohertzina* and other protoconodonts) from the lowest Cambrian (Fortunian, Terreneuvian) and onward (*8*, *9*), with stem-euarthropods (e.g., radiodonts) becoming dominant later on by Cambrian Age 3 (*10*).

Amiskwia sagittiformis Walcott, 1911 from the Burgess Shale shares a similar body plan and nektonic mode of life with chaetognaths due to the presence of paired lateral and tail fins for swimming. While the absence of grasping spines in *Amiskwia* led to a rejection of a relationship with chaetognaths, recent studies demonstrated the presence of an internal jaw apparatus (*11*, *12*), similar to that possessed by gnathiferans. Recent molecular phylogenetic studies have found that chaetognaths and gnathiferans may form a clade (*13*–*15*), Chaetognathifera (*16*). The presence of a gnathostomulid-like jaw in *Amiskwia* has led to competing interpretations of its position in the tree of life, with the lateral fins representing either shared plesiomorphies (*12*, *16*) or convergences (*11*) with those in chaetognaths. This phylogenetic position has important implications for understanding the evolution of the four phyla, Chaetognatha, Gnathostomulida, Micrognathozoa, and Rotifera, such as primitive or secondary miniaturization, benthic versus pelagic lifestyle, and ancestral jaw apparatus morphology.

Here, we describe *Timorebestia koprii* gen. et sp. nov. (Holotype, Fig. 1) from the lower Cambrian Sirius Passet Lagerstätte, North Greenland (Cambrian Stage 3) (*17*). Elemental mapping for carbon using an electron probe microanalyzer (EPMA) allows for certain tissues to be revealed with exceptional clarity (Fig. 1A). *T. koprii* shares with *Amiskwia* the presence of lateral and caudal fins (Fig. 1A and fig. S1, G and H), a distinct head region with long antennae (Figs. 2, A, B, E, and F, and 3) and a jaw apparatus (Fig. 1, D to F; fig. S2; and movie S1) (*18*). We show that *T. koprii* preserves a ventral ganglion (*19*, *20*) in a unique mode through secondary phosphate mineralization (phosphatization) of the lateral neuron somata (Figs. 4 and 5). This organ is shared with chaetognaths to the exclusion of any other living animal group, therefore offering additional evidence placing these fossils on the chaetognath stem (Fig. 5H).

RESULTS

Systematic paleontology

Unranked clade Spiralia Scleip, 1929

Unranked clade Chaetognathifera Bekkouche and Gąsiorowski, 2022

Phylum Chaetognatha Leuckart, 1854 (stem group)

T. koprii gen. et sp. nov.

LSID

urn:lsid:zoobank.org:act:E5E117F9-E6A9-489B-B5C1-668326BC8BCC.

[1]Division of Earth Sciences, Korea Polar Research Institute, 26 Songdomirae-ro Yeonsu-gu, Incheon 21990, Republic of Korea. [2]University of Science and Technology, 217 Gajeong-ro, Daejeon 34113, Republic of Korea. [3]School of Earth Sciences, Palaeobiology Research Group, University of Bristol, Life Sciences Building, 24 Tyndall Avenue, Bristol BS8 1TQ, UK. [4]British Geological Survey, Nicker Hill, Keyworth NG12 5GG, UK. [5]Department of Earth Sciences, University of Oxford, South Parks Road, Oxford OX1 3AN, UK. [6]Natural History Museum of Denmark, University of Copenhagen, Copenhagen DK-1350, Denmark. [7]Department of Biology and Evolution of Marine Organisms, Stazione Zoologica Anton Dohrn, Villa Comunale, 80121 Napoli, Italy. [8]Oxford University Museum of Natural History, Parks Road, Oxford OX1 3PW, UK. [9]Palaeoecosystems Group, Department of Earth Sciences, Durham University, Durham DH1 3LE, UK. [10]Department of Geoscience and Natural Resource Management, University of Copenhagen, Øster Voldgade 10, Copenhagen DK-1350, Denmark. [11]School of Biological Sciences, University of Bristol, Life Sciences Building, 24 Tyndall Avenue, Bristol BS8 1TQ, UK.
*Corresponding author. Email: typark@kopri.re.kr (T.-Y.S.P.); jakob.vinther@bristol.ac.uk (J.V.)

Holotype
MGUH 34286 (Fig. 1 and figs. S1 and S2), Natural History Museum of Denmark, University of Copenhagen.

Referred material
MGUH 34287 (Fig. 2, A and B, and fig. S3), MGUH 34288 (Fig. 2, C to E, and fig. S4), MGUH 34289 (Fig. 2, F and G), MGUH 34290 (Fig. 5, A and B, and fig. S8, A to E), MGUH 34291 (Fig. 6, A to C, and fig. S15, A to D and H to M), MGUH 34292 (fig. S5), MGUH 34293 (fig. S6), MGUH 34294 (fig. S7), MGUH 34295 (Fig. 3 and fig. S8, K to M), MGUH 34296 (fig. S8, F to J), MGUH 34297 (fig. S15, E to G and N to Q), MGUH 34298 (fig. S8, N to P).

Locality and horizon
T. koprii occurs in several horizons at the main Lagerstätte locality (*17*) in Sirius Passet, 82°47.6′N, 42°13.7′W, Peary Land, North Greenland. Collections from which material is derived have been focused on an exposed section that totals 12 m, with collection focused on a particular fossiliferous interval between 5 and 7 m (*21*).

Etymology
Genus name: Timor, (Latin) for causing fear or dread and bestia (Latin), meaning beast. The species name is after Korea Polar Research Institute (KOPRI) for their support of the past, and ongoing, field expeditions to Sirius Passet.

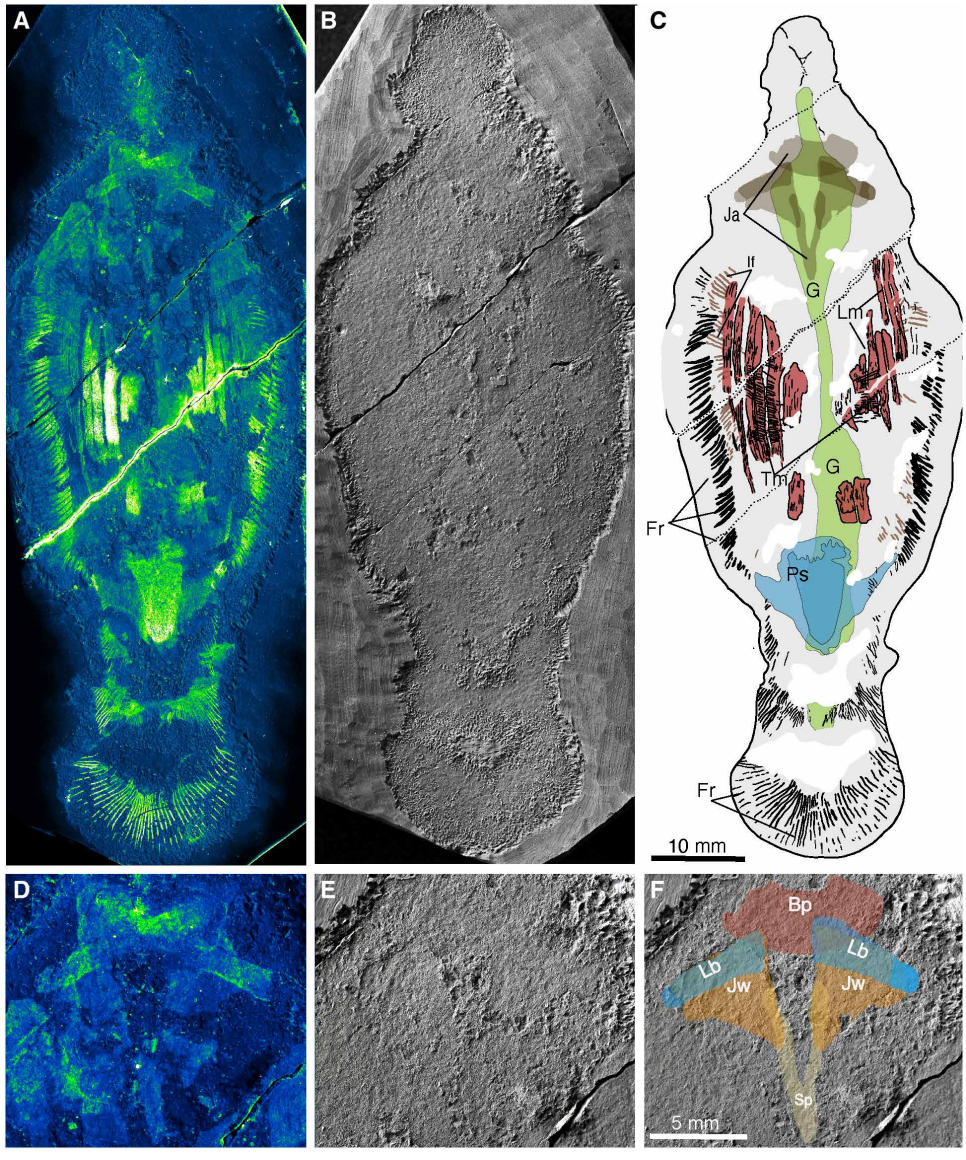

Fig. 1. Holotype (MGUH 34286) of *T. koprii* gen. et sp. nov. (**A** to **C**) Entire specimen. (**D** and **E**) Jaw apparatus in the anterior region of trunk. (A) Wavelength-dispersive x-ray spectrometry (WDS) map of carbon on the specimen surface. (B) Polynomial texture mapping (PTM) visualization using specular enhancement, illuminated from top left. (C) Interpretative drawing. (D) Carbon map of jaw apparatus indicating some indistinct enrichment of carbon within it. (E) PTM image illuminated from top left of jaw apparatus. (**F**) Interpretative drawing of jaw apparatus based on tracing of multiple illumination angles (see movie S1 for visualization of this). Bp, basal plate; Lb, lateral bars; Jw, jaw; Ja, jaw apparatus; G, gut; Tm, transverse muscles; Fr, fin rays; Ps, posterior structure; Lm, longitudinal muscles.

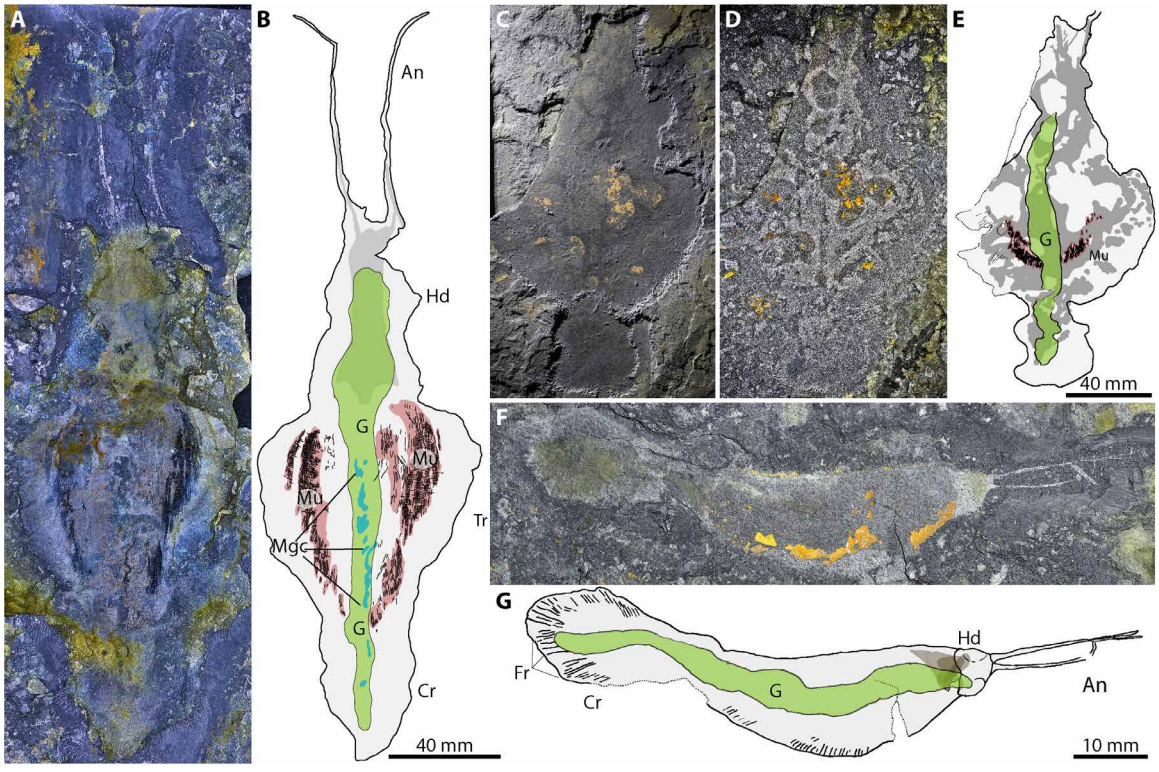

Fig. 2. Additional specimens of *T. koprii* gen. et sp. nov. (**A**) MGUH 34287, the largest preserved individual imaged with high dynamic range (HDR) based on multiple images taken with different incident illumination angles while submerged in water. (**B**) Interpretative drawing. (**C**) MGUH 34288, another very large individual preserving less detail in low angle illumination. (**D**) HDR image. (**E**) Interpretative drawing. (**F**) MGUH 34289, laterally preserved specimen. (**G**) Interpretative drawing. An, antennae; Cr, caudal region; Hd, head; Mu, muscles; Mgc, mineralized gut contents; G, gut; Tr, trunk.

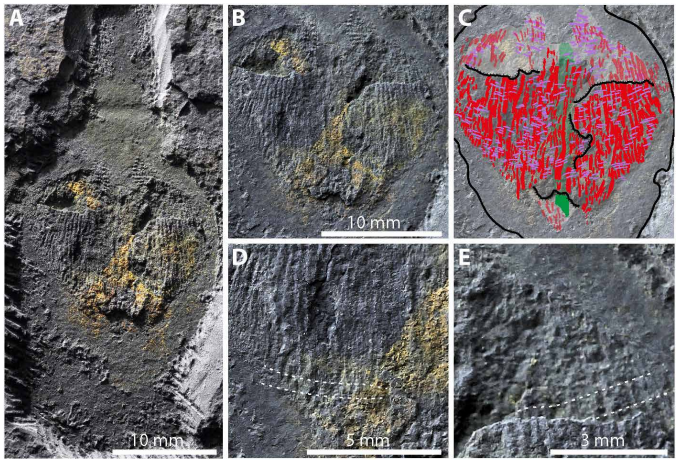

Fig. 3. Musculature in *T. koprii* gen. et sp. nov. MGUH 34295, small specimen preserving phosphatized musculature in association with the ventral ganglion revealing both dorsal and ventral configuration. (**A**) Whole specimen in low angle illumination. (**B**) Close-up of phosphatized musculature, revealing musculature from both dorsal and ventral surfaces due to unequal splitting of the mineralized material. (**C**) Interpretative drawing, highlighting longitudinal musculature (red), transverse/circular musculature (purple), and the gut (green). Hatched lines indicate unequal splitting of the phosphatized musculature. (**D**) Close-up of the mineralized musculature in epirelief; stippled lines trace transverse musculature. (**E**) Close-up of impressions of musculature from the opposite surface in hyporelief, revealing faint impressions of transverse musculature (stippled lines) underneath the longitudinal musculature.

Diagnosis for genus and species

Wide-bodied "amiskwiiform" with lateral fins along most of the trunk length. The body and the lateral fins taper distally and terminate in a well-developed rounded caudal fin. Distinct fin rays are present with no rayless zone separating the trunk and tail fins. Anterior region of trunk tapers markedly into a short head bearing a pair of long antennae, which are about half the length of the body. An internal jaw apparatus in the anterior trunk region consists of a pair of larger subtriangular elements connected by a symphysis, a pair of blunt anterior elements, and a single anterior, presumed ventral/basal, plate. Longitudinal muscles occurring in discrete bands are present in the trunk with additional sparse and delicate outer circular/transverse muscles. The digestive tract extends from the trunk-head transition and terminates anterior to the caudal fin with no septum separating the caudal region from the trunk.

Description

The study included 13 specimens attributed to *T. koprii*, ranging in size from ~22 mm (fig. S15, E to G) to 200 mm in length, or ~290 mm (Fig. 2A) when antennae are included. Variation in degree and mode of preservation due to different levels of decay and secondary mineralization by phosphatization between available specimens result in variable expressions of body extremities and internal organs. Consistent features across specimens allow for identifying and characterizing the body outline (including lateral view; Fig. 2, E and F), fin rays, alimentary tract, jaw apparatus, longitudinal/transverse musculature, and a ventral ganglion. The body is divided

into four distinct regions (Fig. 2, B and F): a pair of anterior antennae about one-third of the total body length (Fig. 2, A, B, E, and F, and fig. S3, A to C), a broad head lacking a neck region, and a dorsoventrally flattened trunk divided into a wide midbody that tapers into a caudal region separated by a longer, constricted margin (Figs. 1 and 2). The head region is often poorly preserved, but is present as a rounded lobe in the best preserved specimens (Fig. 2, A, C, and E, and figs. S3, S6, S7, and S8, F to J). The fin region shows well-developed continuous fin rays along the midbody and caudal region (Fig. 1, A to C, and figs. S1, S5, S6, and S8, A to E), contrasting with *A. sagittiformis* and living chaetognaths in which the lateral and caudal fins are separate. The gut was a tubular structure, widest in the mid body and inferred, based on multiple specimens, to have extended from the rear of the head region and into the caudal region (figs. S1, S3, S4, and S7), terminating anterior to the caudal fin. The position of the mouth opening is unclear.

The holotype (Fig. 1 and figs. S1 and S2) is a medium-sized individual with a complete trunk. The head region is poorly preserved. The preserved body length is 88 mm, while the widest part of the mid body is 33 mm. The trunk widens markedly about 17 mm from the anterior margin of the preserved head and tapers markedly again about 46 mm farther posteriorly into a caudal region. The caudal region (fig. S1G) is ~26 mm long (including the tail fin) and ~13 mm and 18 mm wide at the narrowest and widest part of the fin, respectively. Two specimens are exceptionally large. The largest individual (MGUH 34287; Fig. 2, A and B, and fig. S3) has a body length of ~206 mm and well-defined antennae that are additionally 92 mm long (total length ~298 mm). The posterior region is poorly preserved due to decay, but based on relative proportions between the trunk and the caudal region, as observed in the holotype, the total body length is calculated to slightly surpass 300 mm and is therefore nonetheless largely complete. A second specimen, MGUH 34288 (Fig. 2, C and D), preserves similar body proportions and paired, arcuate phosphate mineralizations in the midbody after musculature and an underlying organ (ventral ganglion, see below). It lacks antennae but has a body length of 178 mm and so are slightly smaller than MGUH 34287.

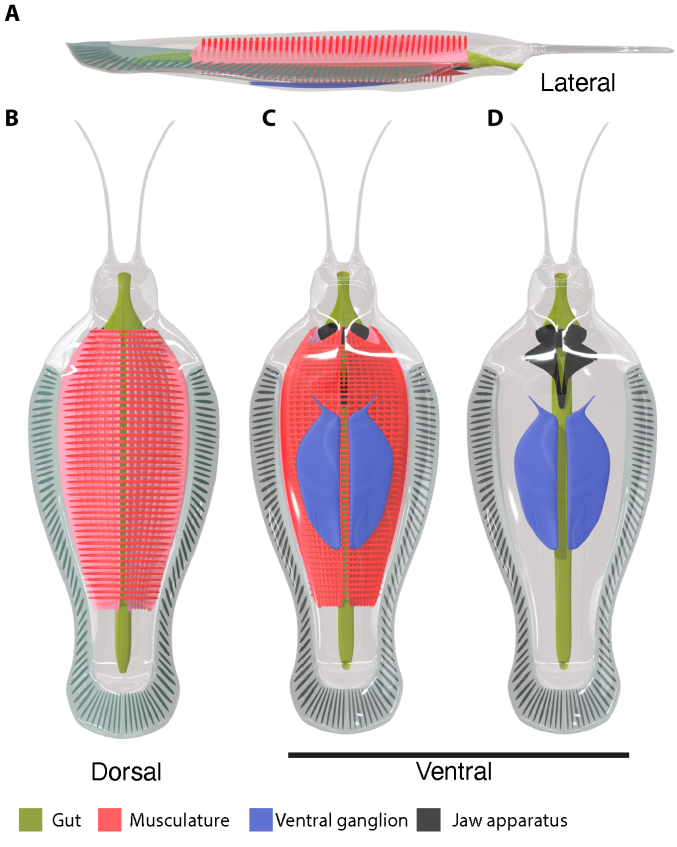

Fig. 4. Digital 3D model of *T. koprii* gen. et sp. nov. Reconstruction showing internal and external anatomy (red, musculature; blue, ventral ganglion; black, jaw apparatus; green, gut). (**A**) Lateral view. (**B**) Dorsal view. (**C**) Ventral view. (**D**) Ventral view excluding musculature.

Several specimens reveal distinct fin rays preserved along the entire trunk (Fig. 1 and figs. S1, A, B, E, and H, S5, A and B, S6, A, C, E, and F, S7, A, B, E, and J, and S8, B, C, and E). Fin rays are stout along the midbody (~350 μm wide in the holotype) becoming longer and narrower in the caudal region (~100 μm wide) (compare fig. S1, G and H). Fin rays are present along most of the trunk (commencing about 10% from the head/trunk junction) and are uninterrupted at the transition into the caudal region (Fig. 1 and figs. S1, A, B, E, and G, and S8, C and E).

Sirius Passet has experienced a higher degree of metamorphic recrystallization (*22*) and volatilization of less recalcitrant organic phases (*23*) than other classic Burgess Shale-type localities limiting some features to those expressed mainly through their relief. We identify faintly impressed structures attributable to a jaw apparatus in the holotype as well as other specimens (Fig. 1, D to F, and fig. S2) traced using multiple, stacked images with different illumination angles (demonstrated in movie S1). At least five elements can be identified: a pair of larger triangular plates that connect posteriorly in a symphysis; a pair of anteriorly placed, transverse, elements that taper laterally with a flattened margin medially and a median anterior plate with anteriorly bulging lateral lobes (Fig. 1, D to F, and fig. S2). The digestive tract is narrow and best observed in the midbody, but it is typically poorly exposed in the caudal and head regions (Fig. 1 and figs. S1F and S3F). Sometimes the digestive tract is locally expanded (fig. S1, D to F) or widened along most of its length (Fig. 6, A to C, and figs. S7, A to G, and S15, A to G), often accompanied by food content. The digestive tract can be traced further into the caudal region where it terminates anterior of the caudal fin (figs. S1, D and E, S3, S4, S6, S7, S8E, and S15, A to G). Anteriorly, it extends into the base of the head and widens into a region containing sclerotized jaw elements, preserved as faint impressions with little reflectivity (Fig. 1D). The digestive tract continues along the midline, preserved sometimes as a reflective film, with some relief and/or as occasional three-dimensional phosphate-derived mineralization (fig. S3F) (*22*). Some specimens preserve food content, dominated by carapaces of the nektonic arthropod *Isoxys* (Fig. 6, A to C, and figs. S4, D and E, S7, C to E, and S15). Their outline is often faint due to preservation within the gut tract of *T. koprii*, which often is preserved with higher reflective carbon. In one specimen (fig. S15, A to D), over five individual *Isoxys* specimens are present. One small specimen contains an *Isoxys* in the jaw region (fig. S15, E to G and N to Q).

The musculature is partly preserved through phosphatization (*22*) (Figs. 3 and 5A and figs. S1, I and J, S3, D and E, and S4F) and as organic strands (Fig. 1A and figs. S1, B and K, S5, B and G, and S6, C and F). The longitudinal muscles form separate ribbons that are

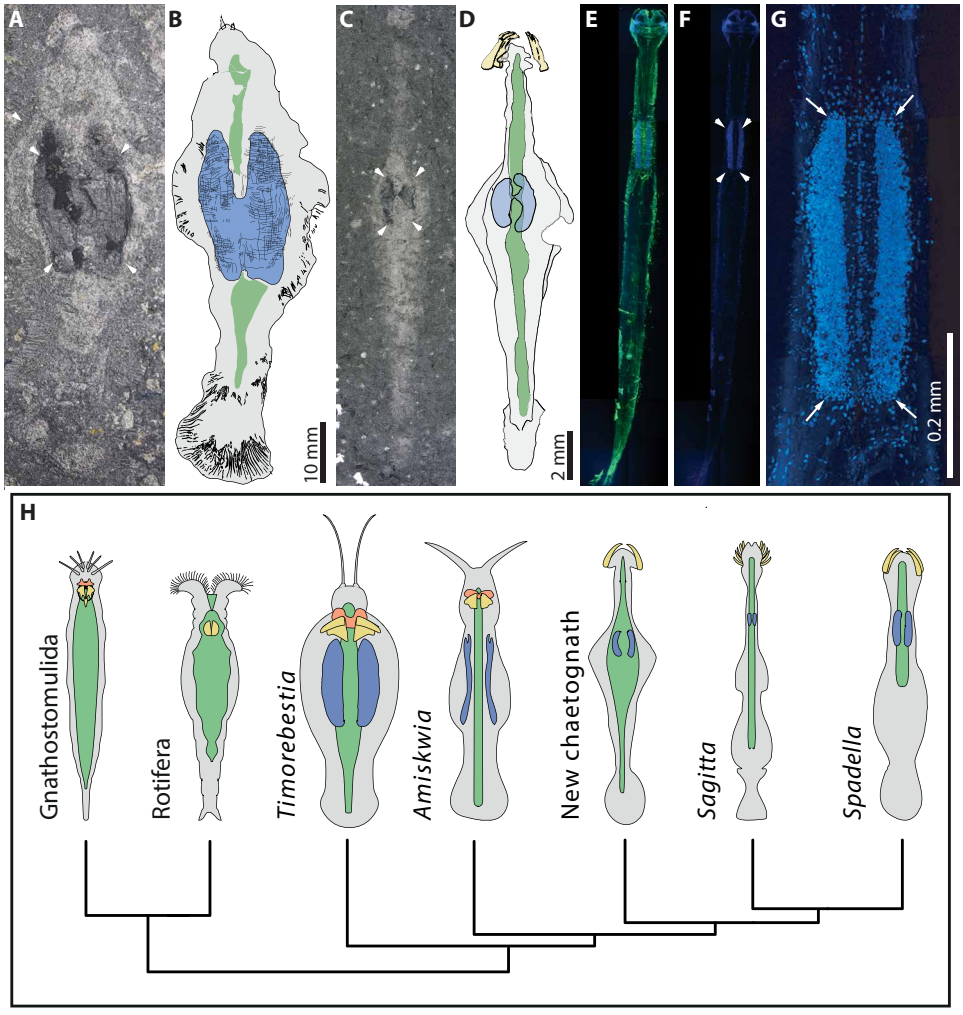

Fig. 5. Ventral ganglion comparisons and phylogenetic relationships. (**A** and **B**) *T. koprii* gen. et sp. nov. MGUH 34290 and an interpretative drawing highlighting the presence of a paired set of bilobed structures (arrowed), mineralized by phosphate interpreted as lateral neuron somata of a ventral ganglion. (**C** and **D**) A small undescribed chaetognath from Sirius Passet, MGUH 34299, preserving the ventral ganglion (arrowed) as paired phosphatized structures. See also fig. S10 for more details of this specimen and details of the grasping spines and additional specimens (figs. S10 and S11). Taphonomic model for preservation of the ventral ganglion is shown in fig. S9. (**E** to **G**) Confocal laser scanning microscope images of the extant chaetognath *Sagitta* sp. (E) Histochemical labeling of nuclei (blue) and α-tubulin (green). (F) Same view as in (E), with only immunolocalization nuclei (blue). (G) Magnified view of the ventral nerve center and the lateral neuron somata (arrowed) enriched in nuclei (blue). (**H**) Summary of phylogenetic analysis (fig. S13 for full analysis) placing *T. koprii* on the chaetognath stem. Schematic reconstructions at the tips indicate relative association of the jaw apparatus, pedal ganglion in rotifers, and ventral ganglion.

densely arranged as observed when phosphatized but are splayed from each other when preserved organically (fig. S6). This variation is likely a consequence of preservation timing, with phosphatization occurring early during post-mortem decay, while organically preserved elements experienced further decay that enabled displacement before compaction. Discrete, transverse musculature is sometimes present as imprints in the mineralized tissues (Fig. 3 and figs. S1I, S3D, S8P). In one specimen, the association between the longitudinal and transverse muscles on both the dorsal and ventral side (Fig. 3, D and E) can be surmised due to muscle preservation by extensive phosphatization in the midbody in which the digestive tract can be seen as an impression, embedded within the two layers (Fig. 3, B and C). The uneven splitting of the rock in which portions of the mineralized material adhered to the counterpart reveals impressions of longitudinal muscles and underlying circular muscles from the opposite surface (Fig. 3E), demonstrating the presence of circular muscles on both sides.

The mineralized musculature is concentrated in the mid-body and varies in extent from a single mass (fig. S6) into a restricted set of bilateral arcuate structures, which appear to be due to conflation with some other organ containing phosphate having this morphology (Figs. 2A and 5A and figs. S3, S4, and S8). Phosphatization of anatomy is common in several taxa from Sirius Passet (*22*), and mostly mineralizes tissues enriched in phosphate in vivo, such as adenosine triphosphate (ATP)–rich musculature (*24*) or the digestive systems of carnivorous taxa (*25*). Neither the nature of the arcuate lateral structures corresponds to the distribution of the more extensive musculature nor do they connect to the digestive

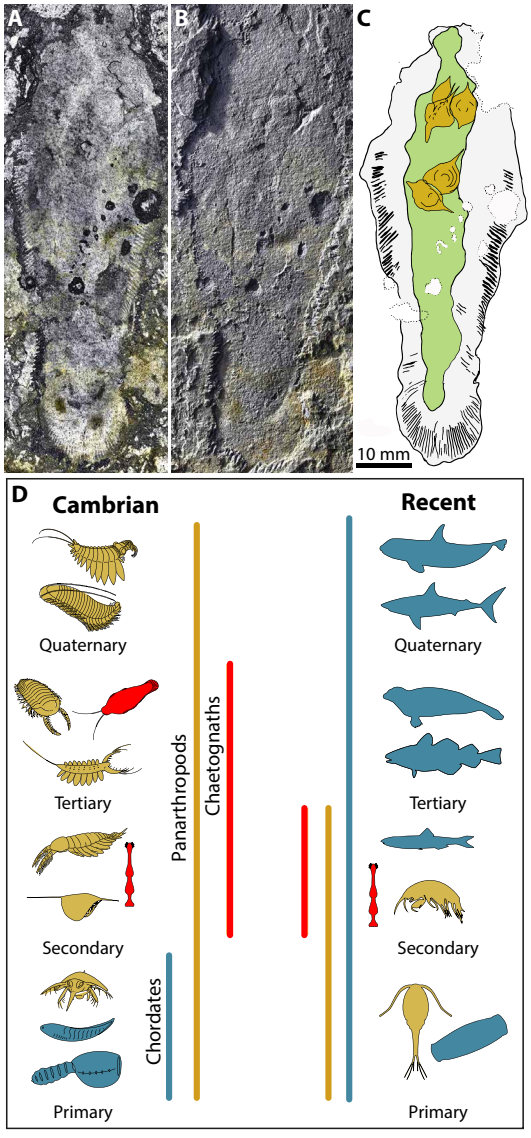

Fig. 6. *Isoxys* predation and evolution of food web tiering. (**A** to **C**) *T. koprii* gen et sp. nov. MGUH 34291, specimen with several specimens of the bivalved arthropod *Isoxys volucris* in its gut. (A) Specimen photographed with reflective light. (B) Specimen photographed with low angle light illuminated from top left. (C) Interpretative drawing (color guide: green, gut; dark yellow, *Isoxys* specimens). (**D**) Schematic presentation of the preserved and inferred components of the pelagic food web in Sirius Passet during the early Cambrian in comparison to modern pelagic food webs, highlighting the downward shift of arthropods and chaetognaths that took place during the Paleozoic as jawed vertebrates evolved to dominate the upper tiers in the food chain.

tract. They are therefore considered to be distinct organs that phosphatized in association with adjacent musculature, which is evident in some specimens where the arcuate mineralizations can be discerned from the musculature by a more featureless texture (fig. S8). The structures resemble the lateral neuron somata of the ventral ganglion of extant chaetognaths (Fig. 5, E to G) (*19*). This organ is composed of serially arranged neurons in which each cell nucleus is localized to the lateral somata (*19*, *20*), apparent when immunohistochemically stained (for DNA) with bisbenzimide (0.5%, Hoechst H 33258) (Fig. 5, E to G). Its unique structure likely aided phosphatization. Cell nuclei contain DNA with a phosphate backbone and could therefore act as a source of phosphate for mineralization when concentrated enough in a tissue such as the lateral neuron somata observed here (fig. S9). This is additionally corroborated by a chaetognath from Sirius Passet with external grasping spines (Fig. 5, C and D, and figs. S10 and S11) shown here for the first time that more closely resembles members of the crown group. Many specimens preserve discrete phosphate mineralizations in their midbody, ranging from a decayed patch (fig. S11) into a set of discrete and paired mineralizations (Fig. 5C and fig. S10, A to D) similar to *T. koprii*. While previous studies have proposed that the pedal ganglion of rotifers is a potential homolog of the chaetognath ventral ganglion (*13*), similar small ganglia are also present in Gnathostomulida (*26*) and Gastrotricha (*27*), suggesting that they are widely distributed among early branching spiralians. These structures differ vastly in their relative size to that present in chaetognaths, and therefore, these massive nervous structures are restricted to members of the chaetognath total group.

Nervous systems typically preserve as carbon-rich reflective structures (*28*, *29*). We note that the reflective structures labeled as "indeterminate organ" in some specimens of *A. sagittiformis* (*11*) conform in appearance and localization to the phosphatized lateral neuron somata observed in *T. koprii* (fig. S12), hence corroborating the identity of these structures as derived from the nervous system and having an affinity with chaetognaths.

DISCUSSION

Because of preservation of tissues as both reflective films and sclerotized structures with relief and through phosphate mineralization, we can reconstruct the anatomical associations of fin rays, musculature, the digestive tract, internal jaw apparatus, and the ventral ganglion (Fig. 4) in *Timorebestia*. *Amiskwia* shares this suite of body plan features with *Timorebestia*, and these taxa have a combination of characters that are not seen in any group of extant gnathiferans and are hereafter referred to as "amiskwiiforms." The affinities of amiskwiiforms have been debated ever since *Amiskwia* was first described (*18*, *30*, *31*) and most recently in terms of their position within the Chaetognathifera (*11*, *12*, *16*). The unique preservation of a ventral ganglion with lateral neuron somata through phosphatization present in both *T. koprii* and the more crownward chaetognath taxon from Sirius Passet described here offer further evidence implying closer affinities of amiskwiids to the chaetognaths (Fig. 5H) than to other chaetognathiferan phyla (*11*). This is corroborated by our phylogenetic analysis (Fig. 5H and fig. S13), wherein *Timorebestia* and *Amiskwia* are the deepest branches in the chaetognath total group. Amiskwiiforms represent a paraphyletic grade of stem-group chaetognaths with a mixture of derived and plesiomorphic traits. The internal jaw apparatus (pair of lateral elements joined by a symphysis and a median basal plate) resembles that of gnathostomulid gnathiferans (*32*), and hence can be surmised to have been the ancestral chaetognathiferan condition. The accessory pair of transverse elements (Fig. 1F and fig. S2) resembles the uncus elements displayed in rotifers (*33*). Modern chaetognaths lack external transverse/circular muscles (*34*), which is otherwise widely observed among several other spiralian phyla. Within the gnathiferan taxa, we see a tendency toward having fewer but stronger circular muscles

among Rotifera (*35*) and Micrognathozoa (*36*). In contrast, Gnathostomulida have numerous, but much thinner circular muscles (*37*–*39*), which is not unlike the condition observed in *T. koprii* (Fig. 3), suggesting that this represents a symplesiomorphic trait shared by gnathostomulids and amiskwiiforms. However, given that the non-chaetognath gnathiferan groups have undergone miniaturization, the discovery of large-bodied stem-lineage fossils of these groups could further clarify the phylogeny, morphological evolution, and the sequence of character acquisition in chaetognathiferans in the future.

The size of the ventral ganglion in *T. koprii* gen. et sp. nov. (Fig. 5A and fig. S8) is noteworthy, as it is larger relative to the body than in living chaetognaths and the fossil taxon with grasping spines from Sirius Passet illustrated here (Fig. 5C and figs. S10 and S11). The ventral ganglion in extant chaetognaths controls the locomotory musculature and integumentary sensory organs (*19*, *40*). The large size of the ventral ganglion in *T. koprii* must therefore have facilitated an expanded locomotory apparatus, although we cannot comment on possible integumentary sense organs on the basis of the features preserved. The lateral fin apparatus in *T. koprii* is highly elaborated, resembling fish and coleoid cephalopods that propel themselves by oscillatory fin movements (modern chaetognaths propel themselves by flexing their body musculature). Such a fin apparatus may explain the need for a higher degree of discrete nervous signaling, which the large ventral ganglion could have accommodated. Other invertebrates with a complex locomotory apparatus also control their movements with an elaborate post-cephalic ganglion. In decabrachiate cephalopods, the oscillatory fins are controlled by large stellate ganglia (*41*).

The extremely large body size offers key insights into the early evolutionary history of chaetognaths (fig. S14). *A. sagittiformis* has a maximum length of 3.5 cm (*11*), making *T. koprii* almost an order of magnitude larger. The large chaetognath *Capinatator praetermissus* Briggs and Caron, 2017 (*42*) from the Burgess Shale is ~10 cm long, similar to the largest living species (*Pseudosagitta gazellae*) (*43*), but only a third of the length of *T. koprii*. The body volume of *T. koprii* (~5.5 log mm^3) places it in the top percentiles among contemporaneous Cambrian pelagic species (*44*, *45*). With their long antennae and complex swimming apparatus, they would likely have been agile pelagic macropredators. This is corroborated by the common occurrence of the pelagic, bivalved arthropod *Isoxys volucris* within the digestive tract of *T. koprii* (Fig. 6, A to C, and figs. S4E and S15).

While modern chaetognaths occupy a role as secondary consumers feeding on zooplankton and small fish, the discovery of *T. koprii* demonstrates that chaetognaths had a stem lineage that included taxa occupying a role higher in the food chain (Figs. 6D and 7). It is noteworthy that chaetognaths are among the oldest pelagic predators, occurring as small shelly fossils (protoconodonts, e.g., *Protohertzina*) in the earliest Cambrian (lower parts of the Fortunian, Terreneuvian), about 538 to 535 million years ago (*9*). Some protoconodonts exhibit more diverse anatomies that depart from the condition observed in extant chaetognaths. *Scoponodus* (*46*) is a unique protoconodont that exhibits a flattened, triangular structure with denticles on one side and a long, projecting element (the bar) bearing some resemblance to the symphysis structure documented in *T. koprii*, although they are still anatomically distinct taxa. The early diversity and occurrence of chaetognaths in small shelly fossil assemblages most likely precedes the colonization of the water column by panarthropods (*10*), which seems to have taken place in the transition from the Cambrian Age 2 to 3 of the early Cambrian (~525 to 522 million years ago). Sirius Passet may therefore reveal a transition between two pelagic evolutionary realms. The inferred trophic displacement of the chaetognath total group could be a result of competitive transposition down the food chain, first by panarthropods. Subsequently, the evolution of jawed vertebrates (Fig. 6D) in the Silurian/Devonian displaced most other invertebrates down the food chain, except for the cephalopods. The discovery of *Timorebestia* may therefore document a window to a pelagic ecosystem that preceded the evolution of nektonic panarthropods—typically encountered in Burgess Shale faunas from the Cambrian Series 2 and Miaolingian—in which large chaetognaths dominated the top of the food chain.

MATERIALS AND METHODS

Material studied

Thirteen specimens of *Timorebestia* gen. nov. were included in this study along with five specimens of a currently undescribed chaetognath. While one specimen of *T. koprii* (MGUH 34289; Fig. 2F) is preserved in lateral view, all other specimens are in dorso-ventral aspect. Apart from the three-dimensional mineralization in some specimens of the lateral somata in the ventral ganglion and neighboring muscles, fossils are usually preserved as thin reflective films, with some relief defining the sclerotized jaw elements and the outline of the gut. All specimens are deposited in the Geological Museum, Natural History Museum of Denmark, University of Copenhagen, prefixed with MGUH. Specimens were cleaned with water and detergents. Some specimens were furthermore cleaned with dilute hydrochloric acid to remove rust on the surface. Mechanical preparation of the fossils was done with an AUTOMEL Electric Engraver (Dong Yang Electric Co.).

Methods

Image acquisition

The fossils were photographed in the laboratory, submerged in water, with a Canon EOS 6D using a Canon EF 100 mm f/2.8L IS USM macro lens. High-angle polarized lighting was used to obtain reflectivity; low-angle (close to horizontal) lighting was used from various orientations to enhance recognition of the low relief of the fossil structure. Specimens were also photographed with low angle lighting dry after having been coated with sublimated magnesium oxide. Images were cropped, adjusted, and enhanced in Adobe Photoshop CS6. The raw images for polynomial texture mapping (PTM) images were acquired using a system (crafted by J. Jung at KOPRI) with lighting from 50 different directions and a Canon EOS 60D equipped with a Canon EF 100 mm f/2.8 USM macro lens. The 50 images were taken for each white-coated specimen, which were converted into a PTM format file. The PTM file was then run in RTI Viewer software, which is freely downloadable at http://culturalheritageimaging.org/What_We_Offer/Downloads/, to acquire enhanced surface details of the fossils.

X-ray elemental mapping

Fossils were gold-coated using a Cressington 108 Auto sputter coater with 10 mA for 70 s. X-ray elemental maps for C, Na, Mg, Al, P, S, Cl, K, Ca, Ti, and Fe were obtained using the JEOL JXA-8530F field emission EPMA at KOPRI, equipped with five wavelength-dispersive x-ray spectrometers (WDS) and an energy-dispersive x-ray spectrometer (EDS). We used an acceleration voltage of 20 kV,

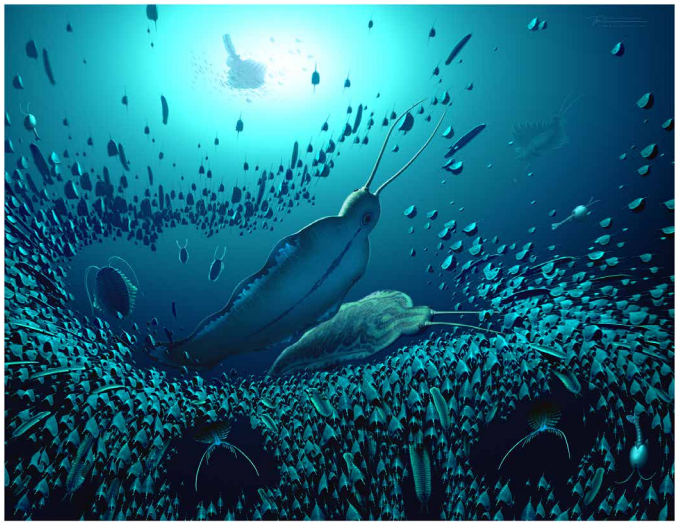

Fig. 7. Reconstruction of *T. koprii* gen et sp. nov. in the pelagic ecosystem preserved in Sirius Passet. Other taxa shown in the foreground are *Kiisortoqia*, *Siricaris*, *Kerygmachela*, *Paulolerminus*, *Kleptothule*, and *Isoxys*. Further in the background is two radiodonts: *Tamisiocaris* and an amplectobeluid. Artwork by Robert Nicholls/BobNichollsArt.

beam current of 200 nA, beam size of 10 to 25 μm, dwell time of 10 to 25 ms, and step size of 15 to 30 μm. WDS and EDS x-ray elemental maps and secondary electron (SE) and backscattered electron (BSE) images were simultaneously obtained via stage mapping. Raw data of x-ray elemental maps and SE and BSE images were imported and processed for brightness and contrast by ImageJ. Three x-ray maps of interest were chosen to make a red-green-blue false color map using ImageJ. Some large specimens were split up due to the size limitation of the EPMA sample stage (90 × 100 mm); a deep groove was made in the back side of the specimen with a fine diamond saw and subsequently cleaved into two pieces. The elemental maps for each specimen piece were acquired separately and then merged in Adobe Photoshop CS6.

Immunohistochemical staining

For confocal laser scanning microscope (CLSM) imaging of the extant chaetognath, *Sagitta* sp. was collected in the Southern Sea of Korea in November 2018 by the KOPRI paleontology team using a plankton net with a mesh size of 100 μm. Specimens were killed and fixed in a 4% formaldehyde solution in artificial seawater with a salinity of 30‰. Nine specimens were preserved at room temperature using 4% paraformaldehyde solution in a phosphate buffer (PB: 0.1 M, pH 7.4) for a duration of 4 hours. Immunohistochemistry was performed on whole mounts of adult specimens using primary and fluorochrome-conjugated secondary antibodies, following standard protocols (*40*). Subsequently, the specimens underwent multiple rinses in phosphate-buffered saline (PBS), followed by pre-incubation in PBS-TX (containing 1% normal goat serum, 0.3% Triton X-100, and 0.05% Na-azide) for 1 hour. Afterward, they were incubated in the primary anti–α-tubulin antibody (mouse monoclonal; Sigma) diluted at a 1:2000 ratio in PBS-TX at room temperature for 12 hours. The specimens were rinsed again for at least 2 hours in multiple changes of PBS and were then incubated with secondary antibodies targeting mouse proteins conjugated to the fluorochrome Cy3 (diluted at 1:500; Jackson ImmunoResearch) for over 4 hours. During the secondary antibody incubations, the specimens were stained with the nuclear dye bisbenzimide (0.5%, Hoechst H 33258) and underwent 2-hour rinsing process in multiple changes of PBS. To minimize autofluorescence, an autofluorescence quenching kit called TrueVIEW (from Vector Lab, a part of Maravai Life Sciences, USA) was used, and the specimens were mounted in Gelmount (Biømeda, USA). Digital images were captured using a Zeiss Axio Imager Z2 fluorescence microscope equipped with a digital camera Axiocam 305 color controlled by Zenblue V 2.5 (Zeiss). The specimens were scanned using Zeiss LSM 800 Confocal Laser Scanning Microscope at KOPRI. The images were generated by stitching together 14 images in the panorama module (Zeiss) to ensure equal optical sections.

Trophic chain

To compare the trophic levels and the position of *T. koprii* in the early Cambrian pelagic system, we identified key pelagic taxa known from the Sirius Passet locality and evaluated their trophic level based on either preserved food content (e.g., *Isoxys* specimens in *T. koprii*) or the functional morphology of feeding structures [e.g., grasping/frontal appendage pincer grasp diameter (*47*) and gnathobase spacing]. The diagram includes an amplectobeluid and a vertebrate-like chordate, which is known from a small number of specimens in Sirius Passet but remains undescribed. These taxa are known from other early Cambrian sites as well, such as Chengjiang in China.

Phylogenetic analysis

See the Supplementary Materials for details of the phylogenetic dataset, characters, and character scores. Phylogenetic analyses were performed in MrBayes 3.2.7 (*48*). Analyses used the mkinf + gamma model (correction for scoring only parsimony informative and rate variation among characters modeled as a gamma distribution). One million generations were requested, and analyses were automatically stopped when the average SD of split frequencies was below 0.01. Convergence was assessed using effective sample size (ESS) (>200) and potential scale reduction factor (PRSF) (~1.0) values for each parameter. Two separate analyses were performed. The first included all taxa, while the second excluded the currently unnamed chaetognath from Sirius Passet.

Supplementary Materials

This PDF file includes:

Supplementary Text
Figs. S1 to S15
Legends for data S1 and S2
Legend for movie S1
References

Other Supplementary Material for this manuscript includes the following:

Data S1 and S2
Movie S1

REFERENCES AND NOTES

1. L. Na, W. Kiessling, Diversity partitioning during the Cambrian radiation. *Proc. Natl. Acad. Sci. U.S.A.* **112**, 4702–4706 (2015).
2. A. M. Bush, R. K. Bambach, Paleoecologic megatrends in marine metazoa. *Annu. Rev. Earth Planet. Sci.* **39**, 241–269 (2011).
3. N. Butterfield, Oxygen, animals and aquatic bioturbation: An updated account. *Geobiology* **16**, 3–16 (2018).
4. G. J. Vermeij, *Evolution and Escalation: An Ecological History of Life* (Princeton Univ. Press, 1993).

5. E. A. Sperling, C. A. Frieder, A. V. Raman, P. R. Girguis, L. A. Levin, A. H. Knoll, Oxygen, ecology, and the Cambrian radiation of animals. *Proc. Natl. Acad. Sci. U.S.A.* **110**, 13446–13451 (2013).
6. N. J. Butterfield, Macroevolutionary turnover through the Ediacaran transition: Ecological and biogeochemical implications. *Geol. Soc. Lond. Spec. Publ.* **326**, 55–66 (2009).
7. J. D. Schiffbauer, J. W. Huntley, G. R. O'Neil, S. A. F. Darroch, M. Laflamme, Y. Cai, The latest Ediacaran wormworld fauna: Setting the ecological stage for the Cambrian explosion. *GSA Today* **26**, 4–11 (2016).
8. J. Vannier, M. Steiner, E. Renvoisé, S.-X. Hu, J.-P. Casanova, Early Cambrian origin of modern food webs: Evidence from predator arrow worms. *Proc. Biol. Sci.* **274**, 627–633 (2007).
9. H. Szaniawski, New evidence for the protoconodont origin of chaetognaths. *Acta Palaeontol. Pol.* **47**, 405–419 (2002).
10. A. C. Daley, J. B. Antcliffe, H. B. Drage, S. Pates, Early fossil record of Euarthropoda and the Cambrian Explosion. *Proc. Natl. Acad. Sci. U.S.A.* **115**, 5323–5331 (2018).
11. J.-B. Caron, B. Cheung, *Amiskwia* is a large Cambrian gnathiferan with complex gnathostomulid-like jaws. *Commun. Biol.* **2**, 164 (2019).
12. J. Vinther, L. A. Parry, Bilateral jaw elements in *Amiskwia sagittiformis* bridge the morphological gap between gnathiferans and chaetognaths. *Curr. Biol.* **29**, 881–888.e1 (2019).
13. A. C. Fröbius, P. Funch, Rotiferan *Hox* genes give new insights into the evolution of metazoan bodyplans. *Nat. Commun.* **8**, 9 (2017).
14. C. E. Laumer, R. Fernández, S. Lemer, D. Combosch, K. M. Kocot, A. Riesgo, S. C. S. Andrade, W. Sterrer, M. V. Sørensen, G. Giribet, Revisiting metazoan phylogeny with genomic sampling of all phyla. *Proc. Biol. Sci.* **286**, 20190831 (2019).
15. F. Marlétaz, K. T. Peijnenburg, T. Goto, N. Satoh, D. S. Rokhsar, A new spiralian phylogeny places the enigmatic arrow worms among gnathiferans. *Curr. Biol.* **29**, 312–318.e3 (2019).
16. N. Bekkouche, L. Gąsiorowski, Careful amendment of morphological data sets improves phylogenetic frameworks: Re-evaluating placement of the fossil *Amiskwia sagittiformis*. *J. Syst. Palaeontol.* **20**, 2109217 (2022).
17. J. S. Peel, J. R. Ineson, The extent of the Sirius Passet Lagerstätte (early Cambrian) of North Greenland. *Bull. Geosci.* **86**, 535–543 (2011).
18. S. Conway Morris, A redescription of the middle Cambrian worm *Amiskwia sagittiformis* Walcott from the Burgess Shale of British Columbia. *Palaontol. Z.* **51**, 271–287 (1977).
19. S. Harzsch, C. H. G. Müller, V. Rieger, Y. Perez, S. Sintoni, C. Sardet, B. Hansson, Fine structure of the ventral nerve centre and interspecific identification of individual neurons in the enigmatic Chaetognatha. *Zoomorphology* **128**, 53–73 (2009).
20. V. Rieger, Y. Perez, C. H. G. Müller, T. Lacalli, B. S. Hansson, S. Harzsch, Development of the nervous system in hatchlings of *Spadella cephaloptera* (Chaetognatha), and implications for nervous system evolution in Bilateria. *Dev. Growth Differ.* **53**, 740–759 (2011).
21. D. A. T. Harper, E. U. Hammarlund, T. P. Topper, A. T. Nielsen, J. A. Rasmussen, T.-Y. S. Park, M. P. Smith, The Sirius Passet Lagerstätte of North Greenland: A remote window on the Cambrian explosion. *J. Geol. Soc. London* **176**, 1023–1037 (2019).
22. M. L. Nielsen, M. Lee, H. C. Ng, J. C. Rushton, K. R. Hendry, J.-H. Kihm, A. T. Nielsen, T.-Y. S. Park, J. Vinther, P. R. Wilby, Metamorphism obscures primary taphonomic pathways in the early Cambrian Sirius Passet Lagerstätte, North Greenland. *Geology* **50**, 4–9 (2022).
23. T. P. Topper, F. Greco, A. Hofmann, A. Beeby, D. A. Harper, Characterization of kerogenous films and taphonomic modes of the Sirius Passet Lagerstätte, Greenland. *Geology* **46**, 359–362 (2018).
24. F. J. Young, J. Vinther, Onychophoran-like myoanatomy of the Cambrian gilled *lobopodian Pambdelurion whittingtoni*. *Palaeontology* **60**, 27–54 (2017).
25. N. J. Butterfield, Leanchoiliaguts and the interpretation of three-dimensional structures in Burgess Shale-type fossils. *Paleobiology* **28**, 155–171 (2002).
26. L. Gąsiorowski, N. Bekkouche, K. Worsaae, Morphology and evolution of the nervous system in Gnathostomulida (Gnathifera, Spiralia). *Org. Divers. Evol.* **17**, 447–475 (2017).
27. A. S.-R. Kieneke, Andreas, in *Handbook of Zoology,* A. Schmidt-Rhaesa, Ed. (de Gruyter, 2015), vol. 3, chap. 1. Gastrotricha.
28. G. D. Edgecombe, X. Ma, N. J. Strausfeld, Unlocking the early fossil record of the arthropod central nervous system. *Philos. Trans. R. Soc. Lond., B, Biol. Sci.* **370**, 20150038 (2015).
29. J. Moysiuk, J.-B. Caron, A three-eyed radiodont with fossilized neuroanatomy informs the origin of the arthropod head and segmentation. *Curr. Biol.* **32**, 3302–3316.e2 (2022).
30. H. B. Owre, F. M. Bayer, The systematic position of the Middle Cambrian fossil *Amiskwia* Walcott. *J. Paleo.* **36**, 1361–1363 (1962).
31. C. Walcott, Middle Cambrian annelids. *Smithson. Misc. Collect.* **57**, 109–144 (1910).
32. M. V. Sørensen, Phylogeny and jaw evolution in Gnathostomulida, with a cladistic analysis of the genera. *Zool. Scr.* **31**, 461–480 (2002).
33. M. V. Sørensen, On the evolution and morphology of the rotiferan trophi, with a cladistic analysis of Rotifera. *J. Zoolog. Syst. Evol. Res.* **40**, 129–154 (2002).
34. C. H. G. Müller, S. Harzsch, Y. Perez, in *Miscellaneous Invertebrates*, A. Schmidt-Rhaesa, Ed. (Walter de Gruyter GmbH & Co KG, 2018), chap. 7, pp. 163–282.
35. M. V. Sørensen, Musculature in three species of *Proales* (Monogononta, Rotifera) stained with phalloidin-labeled fluorescent dye. *Zoomorphology* **124**, 47–55 (2005).
36. N. Bekkouche, R. M. Kristensen, A. Hejnol, M. V. Sørensen, K. Worsaae, Detailed reconstruction of the musculature in *Limnognathia maerski* (Micrognathozoa) and comparison with other Gnathifera. *Front. Zool.* **11**, 71 (2014).
37. M. C. Müller, W. Sterrer, Musculature and nervous system of *Gnathostomula peregrina* (Gnathostomulida) shown by phalloidin labeling, immunohistochemistry, and cLSM, and their phylogenetic significance. *Zoomorphology* **123**, 169–177 (2004).
38. S. Tyler, M. D. Hooge, Musculature of *Gnathostomula armata* Riedl 1971 and its ecological significance. *Mar. Ecol.* **22**, 71–83 (2001).
39. L. Gąsiorowski, N. Bekkouche, M. V. Sørensen, R. M. Kristensen, W. Sterrer, K. Worsaae, New insights on the musculature of filospermoid Gnathostomulida. *Zoomorphology* **136**, 413–424 (2017).
40. S. Harzsch, C. H. Müller, A new look at the ventral nerve centre of *Sagitta*: Implications for the phylogenetic position of Chaetognatha (arrow worms) and the evolution of the bilaterian nervous system. *Front. Zool.* **4**, 14 (2007).
41. D. M. Wilson, Nervous control of movement in cephalopods. *J. Exp. Biol.* **37**, 57–72 (1960).
42. D. E. Briggs, J.-B. Caron, A large Cambrian chaetognath with supernumerary grasping spines. *Curr. Biol.* **27**, 2536–2543.e1 (2017).
43. P. David, The distribution of *Sagitta gazellae* Ritter-Zahony. *Discov. Rep.* **27**, 235–278 (1955).
44. F. A. Smith, J. L. Payne, N. A. Heim, M. A. Balk, S. Finnegan, M. Kowalewski, S. K. Lyons, C. R. McClain, D. W. McShea, P. M. Novack-Gottshall, P. S. Anich, S. C. Wang, Body size evolution across the Geozoic. *Annu. Rev. Earth Planet. Sci.* **44**, 523–553 (2016).
45. N. A. Heim, M. L. Knope, E. K. Schaal, S. C. Wang, J. L. Payne, Cope's rule in the evolution of marine animals. *Science* **347**, 867–870 (2015).
46. Y. Qian, S. Bengtson, *Palaeontology and Bio-Stratigraphy of the Early Cambrian Meishucunian Stage in Yunnan Province, South China*. Fossils and Strata (Universitetsforlaget, 1989), vol. 24, p. 154.
47. G. De Vivo, S. Lautenschlager, J. Vinther, Three-dimensional modelling, disparity and ecology of the first Cambrian apex predators. *Proc. R. Soc. B* **288**, 20211176 (2021).
48. F. Ronquist, M. Teslenko, P. van der Mark, D. L. Ayres, A. Darling, S. Höhna, B. Larget, L. Liu, M. A. Suchard, J. P. Huelsenbeck, MrBayes 3.2: Efficient Bayesian phylogenetic inference and model choice across a large model space. *Syst. Biol.* **61**, 539–542 (2012).
49. T. H. Struck, A. R. Wey-Fabrizius, A. Golombek, L. Hering, A. Weigert, C. Bleidorn, S. Klebow, N. Iakovenko, B. Hausdorf, M. Petersen, P. Kück, H. Herlyn, T. Hankeln, Platyzoan paraphyly based on phylogenomic data supports a noncoelomate ancestry of Spiralia. *Mol. Biol. Evol.* **31**, 1833–1849 (2014).
50. C. E. Laumer, N. Bekkouche, A. Kerbl, F. Goetz, R. C. Neves, M. V. Sørensen, R. M. Kristensen, A. Hejnol, C. W. Dunn, G. Giribet, K. Worsaae, Spiralian phylogeny informs the evolution of microscopic lineages. *Curr. Biol.* **25**, 2000–2006 (2015).
51. S. Gasmi, G. Nve, N. Pech, S. Tekaya, A. Gilles, Y. Perez, Evolutionary history of Chaetognatha inferred from molecular and morphological data: A case study for body plan simplification. *Front. Zool.* **11**, 84 (2014).
52. A. Kieneke, O. Riemann, W. H. Ahlrichs, Novel implications for the basal internal relationships of Gastrotricha revealed by an analysis of morphological characters. *Zool. Scr.* **37**, 429–460 (2008).
53. R. Hochberg, M. K. Litvaitis, Phylogeny of Gastrotricha: A morphology-based framework of gastrotrich relationships. *Biol. Bull.* **198**, 299–305 (2000).
54. J. Girstmair, M. J. Telford, Reinvestigating the early embryogenesis in the flatworm *Maritigrella crozieri* highlights the unique spiral cleavage program found in polyclad flatworms. *Evodevo* **10**, 12 (2019).
55. J. Morris, R. Nallur, P. Ladurner, B. Egger, R. Rieger, V. Hartenstein, The embryonic development of the flatworm *Macrostomum sp*. *Dev. Genes Evol.* **214**, 220–239 (2004).
56. J. Merkel, T. Wollesen, B. Lieb, A. Wanninger, Spiral cleavage and early embryology of a loxosomatid entoproct and the usefulness of spiralian apical cross patterns for phylogenetic inferences. *BMC Dev. Biol.* **12**, 11 (2012).
57. A. Gruhl, Ultrastructure of mesoderm formation and development in *Membranipora membranacea* (Bryozoa: Gymnolaemata). *Zoomorphology* **129**, 45–60 (2010).
58. R. Hochberg, M. K. Litvaitis, A muscular double helix in Gastrotricha. *Zool. Anz.* **240**, 61–68 (2001).
59. D. Eibye-Jacobsen, A reevaluation of *Wiwaxia* and the polychaetes of the Burgess Shale. *Lethaia* **37**, 317–335 (2004).
60. G. Teuchert, The ultrastructure of the marine *gastrotrich Turbanella cornuta* Remane (Macrodasyoidea) and its functional and phylogenetical importance. *Zoomorphologie* **88**, 189–246 (1977).
61. P. Beckers, E. Tilic, Fine structure of the brain in Amphinomida (Annelida). *Acta Zoologica* **102**, 483–495 (2021).
62. J. Guo, L. A. Parry, J. Vinther, G. D. Edgecombe, F. Wei, J. Zhao, Y. Zhao, O. Béthoux, X. Lei, A. Chen, X. Hou, T. Chen, P. Cong, A Cambrian tommotiid preserving soft tissues reveals the metameric ancestry of lophophorates. *Curr. Biol.* **32**, 4769–4778.e2 (2022).
63. C. Nielsen, The triradiate sucking pharynx in animal phylogeny. *Invertebr. Biol.* **132**, 1–13 (2013).

64. A. Filippova, G. Purschke, A. B. Tzetlin, M. C. Müller, Reconstruction of the musculature of *Magelona cf. mirabilis* (Magelonidae) and *Prionospio cirrifera* (Spionidae) (Polychaeta, Annelida) by phalloidin labeling and cLSM. *Zoomorphology* **124**, 1–8 (2005).
65. G. Giribet, G. D. Edgecombe, *The Invertebrate Tree of Life* (Princeton Univ. Press, 2020).
66. M. D. Brazeau, Problematic character coding methods in morphology and their effects. *Biol. J. Linn. Soc.* **104**, 489–498 (2011).
67. L. A. Parry, G. D. Edgecombe, D. Eibye-Jacobsen, J. Vinther, The impact of fossil data on annelid phylogeny inferred from discrete morphological characters. *Proc. R. Soc. B Biol. Sci.* **283**, 20161378 (2016).
68. R. Hochberg, Ultrastructure of feathered triancres in the Thaumastodermatidae and the description of a new species of *Tetranchyroderma* (Gastrotricha: Macrodasyida) from Australia. *J. Mar. Biol. Assoc. U. K.* **88**, 729–737 (2008).
69. B. Lengerer, R. Pjeta, J. Wunderer, M. Rodrigues, R. Arbore, L. Schärer, E. Berezikov, M. W. Hess, K. Pfaller, B. Egger, S. Obwegeser, W. Salvenmoser, P. Ladurner, Biological adhesion of the flatworm *Macrostomum lignano* relies on a duo-gland system and is mediated by a cell type-specific intermediate filament protein. *Front. Zool.* **11**, 12 (2014).
70. V. Malakhov, E. Temereva, Embryonic development of the phoronid *Phoronis ijimai*. *Russ. J. M. Biol.* **26**, 412–421 (2000).
71. C. Nielsen, The phylogenetic position of Entoprocta, Ectoprocta, Phoronida, and Brachiopoda. *Integr. Comp. Biol.* **42**, 685–691 (2002).
72. L. Wu, L. S. Hiebert, M. Klann, Y. Passamaneck, B. R. Bastin, S. Q. Schneider, M. Q. Martindale, E. C. Seaver, S. A. Maslakova, J. D. Lambert, Genes with spiralian-specific protein motifs are expressed in spiralian ciliary bands. *Nat. Commun.* **11**, 4171 (2020).
73. F. P. Fischer, W. Maile, M. Renner, Die Mantelpapillen und Stacheln *von Acanthochiton fascicularis* L. (Mollusca, Polyplacophora). *(Mollusca, Polyplacophora)*. *Zoomorphologie* **94**, 121–131 (1980).
74. H. Chen, L. A. Parry, J. Vinther, D. Zhai, X. Hou, X. Ma, A Cambrian crown annelid reconciles phylogenomics and the fossil record. *Nature* **583**, 249–252 (2020).
75. D. Shu, S. Conway Morris, J. Han, J. F. Hoyal Cuthill, Z. Zhang, M. Cheng, H. Huang, Multi-jawed chaetognaths from the Chengjiang Lagerstätte (Cambrian, Series 2, Stage 3) of Yunnan, China. *Palaeontology* **60**, 763–772 (2017).
76. J. Vinther, L. Parry, D. E. G. Briggs, P. Van Roy, Ancestral morphology of crown-group molluscs revealed by a new Ordovician stem aculiferan. *Nature* **542**, 471–474 (2017).
77. D. L. Feigenbaum, Development of the adhesive organ in *Spadella schizoptera* (Chaetognatha) with comments on growth and pigmentanon. *Bull. Mar. Sci.* **26**, 600–603 (1976).
78. F. Leasi, R. Pennati, C. Ricci, First description of the serotonergic nervous system in a bdelloid rotifer: *Macrotrachela quadricornifera* Milne 1886 (Philodinidae). *Zool. Anz.* **248**, 47–55 (2009).
79. M. Duvert, Y. Bouligand, C. Salat, The liquid crystalline nature of the cytoskeleton in epidermal cells of the chaetognath *Sagitta*. *Tissue Cell* **16**, 469–481 (1984).

Acknowledgments: We thank the Villum Research Station and Station Nord for logistic support. M. Jung helped us in the field camp. We thank the field crew members that participated in expeditions between 2009 and 2018. E. Shim and J. Kim (KOPRI) assisted with imaging work. J. B. Caron sent original images of *Amiskwia* ROM 64013. C. Müller provided original TEM of *Sagitta bipunctata*. We thank M. Cawthorne for assistance with silhouettes shown in Fig. 4. **Funding:** This work was supported by Korea Polar Research Institute (KOPRI) grant funded by the Ministry of Oceans and Fisheries (KOPRI PE23060) (T.-Y.S.P., M.L., J.-H.K., I.A., J.V., and A.T.N.), Geocenter Denmark (D.A.T.H.), Agouron Institute (D.A.T.H.), Carlsberg Foundation (D.A.T.H.), Leverhulme Trust EM-2021-010 (D.A.T.H.), NERC GW4+ DTP NE/L002434/1 (M.L.N.), Postdoctoral fellowship at St. Edmund Hall, Oxford (L.A.P.), and NERC independent research fellowship (grant no. NE/W007878/1) (L.A.P.). **Author contributions:** Conceptualization: T.-Y.S.P. and J.V. Fossil investigation: T.-Y.S.P., J.V., M.L.N., L.A.P., M.V.S., and M.L. Phylogenetic analysis: L.A.P. Food web analysis: M.L.N. Photography: M.L., J.V., T.-Y.S.P., and M.L.N. Immunohistochemistry: T.-Y.S.P. and I.A. Electron microprobe: C.P. and M.L. Digital reconstruction: G.d.V. Interpretative drawing: J.V. Field work: T.-Y.S.P., J.V., M.L., M.L.N., J.-H.K., A.T.N., M.P.S., and D.A.T.H. Writing—original draft: J.V., T.-Y.S.P., and L.A.P. Writing—review and editing: J.V., T.-Y.S.P., L.A.P., M.L.N., M.P.S., M.V.S., and D.A.T.H. Figures: J.V., M.L.N., and L.A.P. Funding acquisition: T.-Y.S.P. and D.A.T.H. **Competing interests:** The authors declare that they have no competing interests. **Data and materials availability:** All data needed to evaluate the conclusions in the paper are present in the paper and/or the Supplementary Materials. Fossil specimens are accessioned to the Natural History Museum of Denmark (SNM) with the accession prefix MGUH 34286-34298 (*T. koprii*, gen. et sp. nov.) and MGUH 34299-34302 (unnamed chaetognath specimen). Images of specimens studied, including EPMA and PTM files, are available through the following DOI: 10.5523/bris.6r7d8clxsjg724z70l84qjdwk. Phylogenetic dataset is available in the Supplementary Materials as a nexus file and is described in detail in Supplementary Text.

Submitted 10 May 2023
Accepted 1 December 2023
Published 3 January 2024
10.1126/sciadv.adi6678